Chemical Engineering Journal 157 (2010) 100–112

Contents lists available at ScienceDirect

Chemical Engineering Journal

journal homepage: www.elsevier.com/locate/cej

Assessment of synthetic zeolite Na A–X as sorbing barrier for strontium in a radioactive disposal facility

R.O. Abdel Rahman [a,*], H.A. Ibrahim [a], M. Hanafy [b], N.M. Abdel Monem [b]

[a] Hot Lab. Center, Atomic Energy Authority of Egypt, P.O. No. 13759, Cairo, Egypt
[b] Chemical Engineering Department, Faculty of Engineering, Cairo University, Egypt

ARTICLE INFO

Article history:
Received 5 August 2009
Received in revised form 23 October 2009
Accepted 27 October 2009

Keywords:
Radioactive waste
Engineered barrier
Disposal
Sorption
Mathematical models

ABSTRACT

The retention of strontium onto synthetic zeolite Na A–X, candidate as backfill material in a near surface disposal facility, was studied using batch and column techniques. In order to investigate the sorption mechanism, the kinetic data were tested using pseudo-first-order, pseudo-second-order, homogenous particle, and intraparticle models. The suitability of the geochemical conditions was preliminarily assessed by conducting equilibrium sorption studies at different pH ranging from 2.0 to 9.0. To optimize the design of the barrier, the effect of the initial concentration on the retention of Sr^{2+} onto the proposed material at three temperatures was investigated. The sorption equilibrium data were analyzed using non-linear Freundlich, Langmuir, and D–R models to evaluate the sorption characteristics and the thermodynamic parameters such as changes in free energy (ΔG), enthalpy (ΔH), and entropy (ΔS) were calculated. To assess the effect of the utilized method to determine the retardation coefficients on the predicted concentration, a simple pulse analytical model was used.

1. Introduction

Strontium-90 is a nuclear fission product that has biochemical behavior similar to calcium. After ingestion with contaminated food about 70–80% of the dose gets excreted. The remaining strontium will be deposited in bone and bone marrow, that might cause bone cancer, cancer of nearby tissues, and leukemia [1]. Significant amounts of strontium are present in spent nuclear fuel, and medical and industrial radioactive wastes. The management of these wastes aims to protect the environment from the waste hazards. Disposal is the last step in radioactive management system that use multibarrier concept to ensure the protection of the environment. Robust selection and designs of these barriers utilize a combination of physical controls and chemical barriers to provide a high level of containment. The main function of the chemical barrier is to retard radionuclide migration [2].

Many researches have been under taken concerning the evaluation of the performance of natural and synthetic zeolite as inorganic ion exchanger for the treatment of radioactive wastes, additive in the immobilization of radioactive waste and as a backfill [3–15]. The wide application of these materials through out the radioactive waste management was based on the high ion exchange capacity that induced from their structure. That is composed of crystalline hydrated aluminosilicate, which is built up of tetrahedral SiO_4 and AlO_4 units bridged by oxygen atoms generating secondary building units. These units may be connected to form rigid three-dimensional structure with tunnel and cavities where the exchange ions are located [14].

One of the most important functional requirements for the backfill barrier is to provide a beneficial aqueous chemical environment so it should have adequate capacity to achieve these requirements. This study is a continuation of our previous work [13,14], at which zeolite Na A–X blend was synthesized and characterized. Cesium sorption and transport behavior were evaluated and the long-term performance of this material was addressed by conducting a quantitative prediction of cesium migration using numerical modeling and the results were compared to that of bentonite. The problem of strontium containment is more complicated than that of cesium due to the lower limit concentration, strontium uptake is very sensitive to the presence of competing ions, especially calcium, and strontium tends to form complexes with complexing agents [16]. In this work, the effect of the initial concentration on the retention of strontium will be evaluated through the assessment of the performance of the synthetic zeolite Na A–X blend. Within this goal, a series of batch and column experiments is conducted and the analyses of their results are utilized to gain insight into the sorption controlling mechanism and the sorption isotherm. Different methods are utilized to determine the strontium retardation coeffi-

* Corresponding author. Tel.: +20 161404462; fax: +20 24620796.
E-mail addresses: karimrehab1@yahoo.com, alaarehab@yahoo.com (R.O.A. Rahman).

1385-8947/$ – see front matter © 2009 Elsevier B.V. All rights reserved.
doi:10.1016/j.cej.2009.10.057

Nomenclature

b	Langmuir constant related to the energy of sorption
C_{pi}	intraparticle intercepts at stage i
C_x	concentration of metal ion in solution at state x [mg/l]
D_L	hydrodynamic dispersion coefficient [m^2/s]
D_r	particle diffusion coefficient [m^2/s]
D_x	particle size at x fraction [mm]
E	energy of sorption estimated by D–R model [kJ/mol]
k_1	pseudo-first-order rate constant [min^{-1}]
k_2	pseudo-second-order rate constant [g/mg min]
k_c	equilibrium constant
K_d	distribution coefficient
K_f	Freundlich constant indicative of the relative adsorption capacity [mg/g]
K_{pi}	intraparticle rate constant [mg/g $min^{0.5}$]
m	weight of the adsorbent [g]
n	Freundlich constant indicative of the relative sorption capacity
Q^o	Langmuir saturation capacity [mg/g]
q_x	amount of metal ions sorbed onto zeolite Na A–X at state x [mg/g]
q_m	maximum amount of ion that can be sorbed onto unit weight of zeolite [mg/g]
R	gas constant [8.314 J/mol K]
R^2	correlation coefficient
R_f	retardation coefficient
R_L	equilibrium parameter constant
T	absolute temperature [K]
U	number of effluent pore volume
v	mean pore water velocity [m/s]
V	volume of solution [l]
x	distant traveled in flow direction [m]
X	fraction attainment of equilibrium at time t
ΔG^o	Gibbs free energy [kJ/mol]
ΔH^o	enthalpy change [kJ/mol]
ΔS^o	entropy change [J/mol K]

Symbols

β	constant related to sorption energy [mol^2/kJ^2]
ε	polanyi potential
θ	porosity
δ	thickness of the liquid film
ρ_d	bulk density

Suffix

e	equilibrium state
i	stage of the intraparticle model
o	initial state
t	time variant state

cient and a simple analytical model is used to predict the strontium concentration.

2. Materials and methods

Fly ash, obtained from an Egyptian thermal electric power station as by-product, was used to prepare zeolite Na A–X blend by alkaline fusion and SiO_2 extraction method at laboratory scale. The preparation procedure, characterization of fly ash and the produced zeolite Na A–X were illustrated elsewhere [12–14]. The chemical composition of the fly ash and the elemental analysis of the prepared zeolite are summarized in Table 1a, the physical properties of the zeolite are presented in Table 1b. The stock solutions of Sr^{2+} were prepared in simulated groundwater; the composition of the groundwater is presented in Table 2 [13]. Batch and column techniques were utilized to investigate the sorption and dispersion characteristics of Sr^{2+} onto the proposed backfill. Both batch and column experiments were carried out in triplicates and the mean values were presented.

2.1. Batch technique

A series of batch experiments was utilized to study the effect of contact time and initial Sr^{2+} concentration on the sorption kinetics, investigate the effect of groundwater pH on the sorption process, and to analyze the sorption isotherm data.

2.1.1. Kinetic studies

Kinetic batch studies were performed at ambient temperature (298 K) using three initial concentrations of 50.0, 100.0, and 150.0 mg/l for Sr^{2+} sorption onto zeolite Na A–X blend at mean groundwater pH of 7.0. For these investigations 0.1 g of the studied zeolite was immersed in 100.0 ml Sr^{2+}-groundwater solution under constant shaking using thermostatic shaker. A fixed volume of (2 ml) of the aliquot was withdrawn at predetermined time intervals while the solution was being continuously shacked, thus the ratio of the solution volume to the zeolite weight does not change from its initial value. The withdrawn aliquot was centrifuged to separate the solid from the liquid phase. The obtained clear liquid phase was diluted to an appropriate concentration range for elemental analysis using atomic absorption spectrophotometer (Buck scientific model VGP 210). The amount of sorbed Sr^{2+} at any time q_t (mg/g) was calculated as follow:

$$q_t = (C_o - C_t)\left(\frac{V}{m}\right) \quad (1)$$

where C_o and C_t are the initial and time variant concentrations of Sr^{2+} in groundwater (mg/l), V the volume (l) and m the weight (g) of zeolite.

2.1.2. Effect of groundwater pH

The suitability of the geochemical condition was preliminarily checked by examining the pH range at which the maximum sorption of Sr^{2+} ions take place on the studied zeolite and comparing this range with the mean groundwater pH (pH = 7). Within this context, a series of test tubes each containing 0.1 g zeolite immersed in 100.0 ml of Sr^{2+}-groundwater solution at fixed temperature (298 K) were utilized. The initial pH was adjusted to value ranging from 2.0 to 9.0 using diluted solution of sodium hydroxide or hydrochloric acid. The kinetic investigations showed that

Table 1a
Chemical composition of fly ash and synthetic zeolite Na A–X blends.

Composition (wt%)	CaO	SiO_2	Al_2O_3	Fe_2O_3	MgO	SiO_3	Na_2O	K_2O	Others	pH
Fly ash	6.1	43.81	23.18	0.01	0.8	–	0.87	2.73		
Composition (wt%)	Na	Al	Si	Ca	Ti	Mg	Fe	S	K	P
Zeolite Na A–X	27.79	33.41	38.34	0.067	0.081	0.062	0.01	0.002	0.056	0.004

Table 1b
Physical properties of the prepared zeolite.

Properties	Value
Porosity (θ)	0.6
Bulk density (ρ_d) (g/cm^3)	0.8
Mean grain size, D_{50} (mm)	0.38
D_{10} (mm)	0.25
D_{60} (mm)	0.4

the studied sorption process had reached equilibrium in 90 min, so the tubes were shacked for 3 h to ensure that the reaction attained equilibrium. Then the suspension was centrifuged to separate the solid from the liquid phase, the clear liquid phase was analyzed using the same mentioned procedure. The distribution coefficient K_d, was calculated using the following equation:

$$K_d = \left[\frac{C_o - C_e}{C_e}\right]\frac{V}{m} \times 10^3 \quad (2)$$

where C_e is the equilibrium concentration of Sr^{2+} in groundwater (mg/l).

2.1.3. Sorption isotherm

For isotherm studies, 100 ml of Sr^{2+}-groundwater solution of varying initial concentrations (100–1000 mg/l) were shacked continuously for 3 h with 0.1 g of zeolite at initial pH of 7 (mean groundwater pH) at three different temperatures 298, 313, and 333 K. This temperature range was selected to be in consistent with the temperature in intermediate level waste disposal for short lived radionuclides that can reach a maximum of 353 K around the time of backfilling, but, in the post-closure period, would more typically be between 323 and about 308 K between the core and the edges of disposal vaults [17]. After equilibrium, the suspension was centrifuged and analyzed and the equilibrium Sr^{2+} concentration retained in the zeolite (mg/g) was calculated using the following equation:

$$q_e = (C_o - C_e)\left(\frac{V}{m}\right) \quad (3)$$

2.2. Column technique

Column experiments were conducted in vertical down flow column with 4.5 cm inner diameter and 30.0 cm length to study the transport phenomena under saturated conditions. The columns were packed with zeolite Na A–X blend (with 0.8 bulk density, 0.6 porosity, and 250 μm particle size). Groundwater containing initial Sr^{2+} concentration of 50–150 mg/l was utilized as the liquid phase. The groundwater was initially permeated through the column to ensure that the steady state conditions were achieved before introducing Sr^{2+}, the inlet flow rate was 3.0 ml/min [13].

3. Results and discussion

3.1. Sorption kinetics

3.1.1. Effect of contact time

The effect of contact time was performed at initial Sr^{2+} concentrations of 50.0, 100.0, and 150.0 mg/l at ambient temperature (298 K) for the sorption onto zeolite Na A–X blend, the results were shown in Fig. 1a. It is clear that the amount of sorbed Sr^{2+} increases with increasing the initial concentration of Sr^{2+}. Also, the sorbed amount sharply increases with time in the initial stage (0–30 min), and then gradually increases to reach an equilibrium value in approximately 90 min. A further increase in the contact time had a negligible effect on the amount of Sr^{2+} sorbed. The rapid Sr^{2+} sorption portion might be attributed to the availability of large number of vacant surface sites for sorption and after that time interval; the remaining vacant sites become more difficult to be occupied due to the repulsive forces between the solute molecules on the solid and bulk phases [18]. According to these results, the contact time was fixed at 3 h for the isotherm experiments to make sure that the equilibrium was reached.

Table 2
Chemical composition of synthetic groundwater.

TDS (mg/l)	Soluble cations (ppm)				Soluble anions (ppm)		
	K^+	Na^+	Mg^+	Ca^{++}	Cl^-	SO_4^-	HCO_3^-
1.05	23	149	13	74	137	317	272

3.1.2. Sorption kinetics analysis

The results obtained from the effect of contact time on the sorption process, illustrated in Fig. 1a, were used to gain insights into the nature of the sorption process of Sr^{2+} onto zeolite Na A–X blend, to identify the controlling sorption mechanism and to determine the kinetic parameters that are of importance for designing and modeling contaminant transport through engineered barriers. Four kinetic models, pseudo-first-order, pseudo-second-order, intraparticle diffusion and homogenous particle diffusion [19–24], were used to analyze the experimental data using linear regression scheme.

The analysis of the experimental data using pseudo-first-order kinetic equation has been conducted; this model has been widely used to analyze the sorption kinetics. It describes the sorption rate based on the sorption capacity and assumes that the reaction rate is limited by only one process or mechanism on a single class of sorbing sites and that all sites are of the time dependent type [25]. The model equation is given by:

$$\log(q_e - q_t) = \log q_e - \frac{k_1}{2.303}t \quad (4)$$

where q_e and q_t (mg/g) are the amount of metal ion sorbed onto zeolite Na A–X at equilibrium and at time t, respectively and k_1 is the pseudo-first-order rate constant (min^{-1}). The parameters q_e and k_1 are determined by applying the linear regression procedure for Eq. (4). Fig. 1b shows the results of this analysis; the obtained straight lines suggest the applicability of pseudo-first-order kinetic equation to fit the experimental data. By comparing the values of theoretically calculated equilibrium sorption capacities, q_e, with the apparent experimental sorption capacities, a considerable deviation between these values is noticed as shown from Table 3 and Fig. 1a. This deviation indicates that it is not appropriate to use pseudo-first-order kinetic equation to represent the sorption of Sr^{2+} onto zeolite Na A–X blend for the entire sorption period. The experimental data obtained within the initial stage of the sorption process (30 min) were further fitted to pseudo-first-order as shown in Fig. 1c. By comparing the values of the correlation factor (R^2), as indicated in Fig. 1b and c, higher values are observed for fitting the experimental data within the first 30 min to pseudo-first-order equation. This indicates that the sorption process within this time period might be proceeded by diffusion through the boundary [26,27].

Pseudo-second-order chemisorption kinetic rate equation is derived on the basis of the sorption capacity of the solid phase [28]. It assumes that the rate of sorption is directly proportional to the number of active surface sites and that the rate limiting step may be a chemical sorption involving valence forces through sharing or exchange of electrons between the adsorbent and the adsorbate [29–31]. The linear form of the model is expressed as:

$$\left(\frac{t}{q_t}\right) = \left(\frac{1}{k_2 q_e^2}\right) + \left(\frac{1}{q_e}\right)t \quad (5)$$

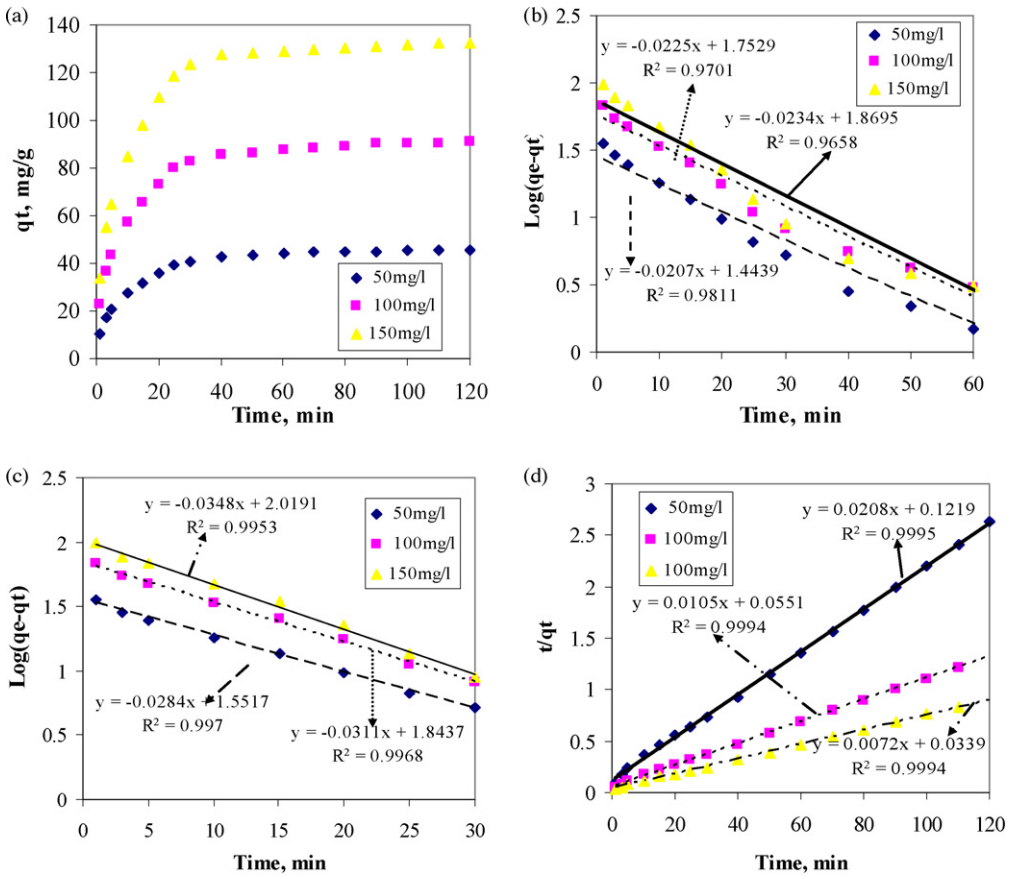

Fig. 1. Kinetic modeling of the sorption of Sr^{2+} onto the prepared zeolite Na A–X blend at 289 K. (a) The effect of contact time at different initial Sr^{2+} concentrations. (b, c) Pseudo-first-order kinetics for a sorption period of 60 min and initial stage (30 min) respectively. (d) Pseudo-second-order kinetics.

where k_2 is the rate constant of pseudo-second-order equation (g/mg min). The product $k_2 q_e{}^2$ is the initial sorption rate represented as $h = k_2 q_e^2$. In accordance to the result of the analysis of experimental data using the pseudo-second-order equation (Table 3 and Fig. 1d), it was found that the relation is linear, and the values of the correlation coefficient suggests a stronger correlation between this equation and the experimental data. The correlation coefficients have extremely high values (>0.999), and its calculated equilibrium sorption capacity (q_e) is consistent with the experimental data. The examination of the initial sorption rate (h) values indicates that the initial sorption rate increase as the initial concentration increases where the rate constants decreased markedly with increasing the initial concentration. Similar phenomena are observed for the sorption of Pb onto tuff zeolite and for the sorp-

Table 3
Results of the kinetic studies of Sr^{2+} sorbed onto zeolite Na A–X.

Model	Time scale	Equation	Model parameter	Concentration		
				50 mg/l	100 mg/l	150 mg/l
Pseudo-first-order	Entire range	$\log(q_e - q_t) = \log q_e - \frac{k_1}{2.303} t$	q_e (mg/g)	27.8	65.6	74.01
			k_1 (min^{-1})	0.047	0.052	0.054
			R^2	0.98	0.97	0.96
	To 30 min		q_e (mg/g)	35.6	69.77	104.
			k_1 (min^{-1})	0.065	0.071	0.08
			R^2	0.997	0.996	0.995
Pseudo-second-order	Entire range	$\left(\frac{t}{q_t}\right) = \left(\frac{1}{k_2 q_e^2}\right) + \left(\frac{1}{q_e}\right) t$	q_e (mg/g)	48.08	95.24	138.89
			k_2 (g/mg min)	0.003	0.002	0.0015
			h (mg/g min)	8.20	18.15	29.50
			R^2	0.999	0.999	0.999
Homogenous particle diffusion	Entire range	$-\ln(1 - X) = \frac{3DC_o}{r_o \delta q_o} t$ $r_o = D_{50}$	Not valid			
	Entire range	$-\ln(1 - X^2) = \frac{3D_r \pi^2}{r_o^2} t$ $r_o = D_{50}$	D (m^2/s)	2.64×10^{-12}		
			R^2	0.98	0.97	0.97
Intraparticle	To 20–25 min	$q_t = K_{pi}\sqrt{t} + C_{pi}$	K_{p1} (mg/g min$^{0.5}$)	8.49	17.52	26.12
			C_{p1}	0.0	0.0	0.0
			R^2	0.961	0.933	0.934
	From 20 to 25 min		K_{p2} (mg/g min$^{0.5}$)	1.08	1.54	1.55
			C_{p2}	35.09	75.11	116.54
			R^2	0.87	0.95	0.90

tion of Cs and Sr onto zeolite A [4,32]. From these results, it could be concluded that the sorption of Sr^{2+} onto zeolite Na A–X blend obeys pseudo-second-order kinetic equation for the entire sorption period and thus supports the assumption that the sorption is due to chemisorption, through sharing of electrons or covalent forces, until the surface active sites are fully occupied thereafter Sr^{2+} diffuses into the zeolite for further interactions and/or reactions [29–31,33–38].

There are different stages in the sorption process by porous adsorbents including: bulk diffusion, film diffusion, intraparticle diffusion and physical and/or chemical reaction [14]. One or more of the above-mentioned stages may control the sorption process. Bulk diffusion could be ignored if sufficient mixing speed is achieved. Both pseudo-first- and second-order equations include all steps of sorption, in order to identify the controlling sorption mechanism; the kinetic data were analyzed by homogenous particle model equations, this model assumes that the rate determining step of sorption could be described by either film diffusion, at which the ions diffuse through the liquid film surrounding the particle Eq. (6), or by particle diffusion at which the ions diffuse into the sorbent beads Eq. (7) [39].

$$-\ln(1-X) = \frac{3DC_o}{r_o \delta q_o} t \quad (6)$$

$$-\ln(1-X^2) = \frac{3D_r \pi^2}{r_o^2} t \quad (7)$$

where D is the diffusion coefficients in the liquid phase (m^2/s), and D_r is the particle diffusion coefficient (m^2/s), X the fraction attainment of equilibrium, δ is the film thickness and r_o is the radius of the sorbent particle. The results of the analysis of the kinetic data by homogenous particle model equations are illustrated in Fig. 2a and b and the calculated parameters are listed in Table 3. The plots of $-\ln(1-X)$ versus contact time is a linear relationship that does not pass through the origin. This means that the film diffusion is not the controlling sorption mechanism. Where the plots of $-\ln(1-X^2)$ is a linear relationship that pass through the origin. These results revealed that the particle diffusion might be the controlling sorption mechanism at all studied Sr^{2+} concentrations. The values of the slope at the three studied concentration are constant which shows that the diffusion coefficient is independent on the initial concentration. The particle diffusion coefficient was calculated form the slope of $-\ln(1-X^2)$ versus time as presented in Table 3, the magnitude of the diffusion coefficients dependent on the nature of the mechanism that control the sorption process. For physical sorption, the value of the diffusion coefficient ranges from 10^{-6} to $10^{-9}\ m^2/s$ and for chemisorption the value ranges from 10^{-9} to $10^{-17}\ m^2/s$ the difference in these values is due to the fact that in physical sorption the bounds of the molecules are weakly and can easily break and the molecules can migrate, whereas for chemisorption the molecules are strongly bound and mostly localized [39]. The tabulated value of the diffusion coefficient is in the order of $10^{-12}\ m^2/s$ which confirms the result obtained from the analysis of the data to pseudo-second-order that the sorption process is chemisorption process. The obtained diffusion coefficient is in the same range of other reported study for backfill material composed of a mixture of clay and crushed rock [40].

Intraparticle diffusion model is based on Weber and Morris theory, at which the sorption varies almost proportionally with $t^{1/2}$ as follow:

$$q_t = K_{pi}\sqrt{t} + C_{pi} \quad (8)$$

where K_{pi} the rate parameter of stage i ($mg/g\ min^{0.5}$). C_{pi}, the intercept of stage i, gives an idea about the thickness of boundary layer, i.e., the larger the intercept, the greater the boundary layer effect [18]. Fig. 2c illustrates the analysis of the experimental data to intraparticle equation, the plots of q_t versus $t^{0.5}$ shows the existence of two portions representing two different stages in the sorption process. The initial portion is due to surface sorption and rapid external diffusion (boundary layer diffusion). The second linear portion is a high and gradual sorption stage where the intraparticle diffusion is the controlling mechanism [27]. The results presented in Fig. 2d revealed that the initial portion of the sorption process was completed in the range of 20–30 min and the gradual portion was then attained. The existence of the gradual portion (that does not pass through the origin) indicates that there is some degree of boundary layer control and suggest that the intraparticle diffusion is not the only controlling mechanism. The experimental data within the first portion were further analyzed using the intraparticle diffusion equation. The values of the rate constants at the first stage were given in Table 3. For the second portion, the value of the intercept of the second stage gives an idea about the thickness of the boundary layer, from the tabulated values it is shown that the intercept increase as the concentration increase, this mean that as the concentration increase the boundary layer effect will be greater [18,41]

3.2. Effect of groundwater pH

Change in the environmental conditions such as groundwater pH might affect the sorption process. This usually causes marked changes in the retention of contaminants onto the engineered barriers. The suitability of the geochemical conditions was preliminarily assessed by conducting equilibrium sorption studies at different pH ranging from 2.0 to 9.0. It was observed that the values of the Sr^{2+} distribution coefficients (k_d) increases as the groundwater pH increases and nearly reaches a plateau at pH 6 (Fig. 3a). This reflects that the material is showing a reasonable retention performance at the mean groundwater pH (pH = 7). This effect of pH is observed markedly in mineral oxides such as silica and alumina [42]. The low values of cation sorption at acidic groundwater might be attributed to the fact that at low pH the barrier surface becomes more positive or less negative because of proton sorption from groundwater onto the charged sites. Also, at acidic groundwater the solubility of zeolite constituents is noticed and so there will be relatively small number of available sites [14]. The enhanced sorption of Sr^{2+} with increasing pH value is related to the hydroxyl group at the zeolite surface that might be coordinated by two similar atoms (two Si or two Al) or different ones (one Si and one Al) this lead to the existence of different surface hydroxyl group properties and therefore sorption affinity. Three main reactions might be responsible for the sorption of bivalent cations at the prepared zeolite:

$$\equiv OH + Sr^{2+} \Leftrightarrow \equiv O^- Sr^{2+} + H^+ \quad (9)$$

$$2(\equiv OH) + Sr^{2+} \Leftrightarrow (\equiv O^-)_2 Sr^{2+} + 2H^+ \quad (10)$$

$$\equiv OH + Sr^{2+} + H_2O \Leftrightarrow \equiv O^- Sr^{2+} + OH + 2H^+ \quad (11)$$

As indicated in the above equations the interaction of Sr^{2+} releases hydrogen ions so the increase of groundwater pH will favor the sorption of Sr^{2+}. Also, there is a possible correlation between the complexation reaction of surface hydroxyl groups and the ability to form hydrated complexes by Sr^{2+} cations as seen from the analogy between the reactions [43].

$$Sr^{2+} + H_2O \Leftrightarrow Sr^{2+} + OH + H^+ \quad (12)$$

$$Sr^{2+} + \equiv OH \Leftrightarrow O^- Sr^{2+} + H^+ \quad (13)$$

3.3. Sorption isotherm analysis

The waste packages and the backfill are disposed in the disposal facility. Under natural evolution scenario, the engineered barriers

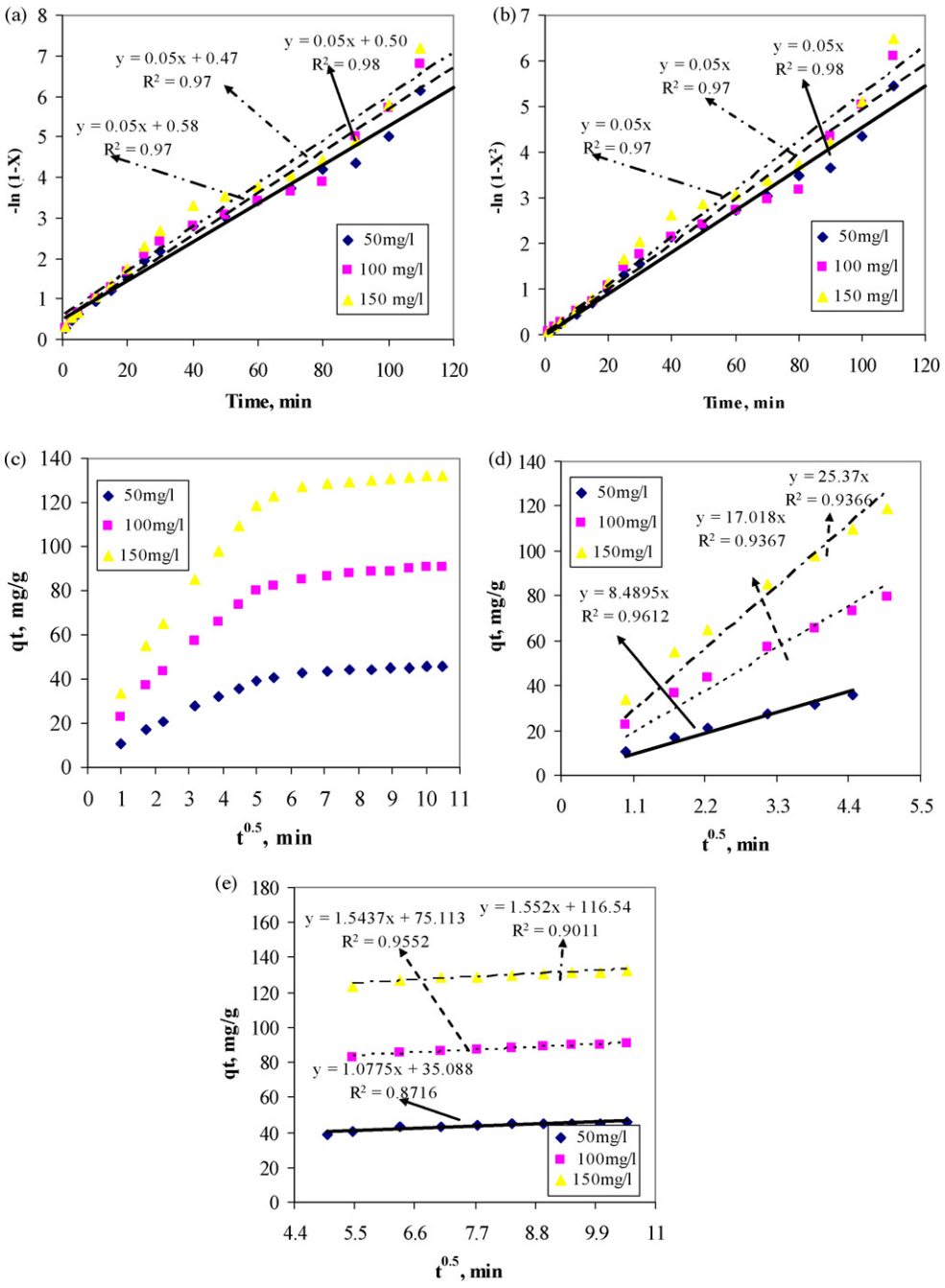

Fig. 2. Evaluation of the controlling sorption mechanism by using homogenous particle diffusion equation (a, b) and intraparticle diffusion equation (c–e).

degrade through different possible feature, event and process and the disposed radionuclides start to diffuse from the waste package into the surrounding pore water [13]. The transfer of these radionuclides from the pore water to the backfill is an important process that reduces the radionuclides release to the environment. To optimize the design of the barrier, a proper understanding of the sorption isotherm is needed that describe the retention of the radionuclides on the barrier at different initial concentrations. Fig. 3a illustrates the effect of initial concentration on the retention of Sr^{2+} onto the zeolite Na A–X blend at the three studied temperatures; the batch distribution coefficient (K_d), as a general ability of the barrier to remove the radionuclides, was utilized. The figure shows that at high initial concentration ranges (higher than 500 mg/l) the effect of ambient temperature on the assessment of the distribution coefficients is negligible. On the other hand for lower initial concentration, as the ambient temperature increases the distribution coefficients will increase. Accurate comparison of the distribution coefficients requires identical experimental conditions in terms of volume to mass ratio, equilibrium solution composition, material, temperature, etc because all of these factors can affect the value of K_d. So it will be unreliable to provide a comparison with other reported studies for the retention in terms of K_d.

The examination of the relationship between Sr^{2+} concentration remaining in the groundwater and those sorbed on the synthetic zeolite Na A–X blend show a concave curve which suggest a progressive saturation of the solid (Fig. 3b). Linear regression was utilized to fit the experimental data to the linear form of Freundlich, Dubinin–Radushkviech (D–R), and Langmuir isotherm equations, and the least square method has been applied to determine the

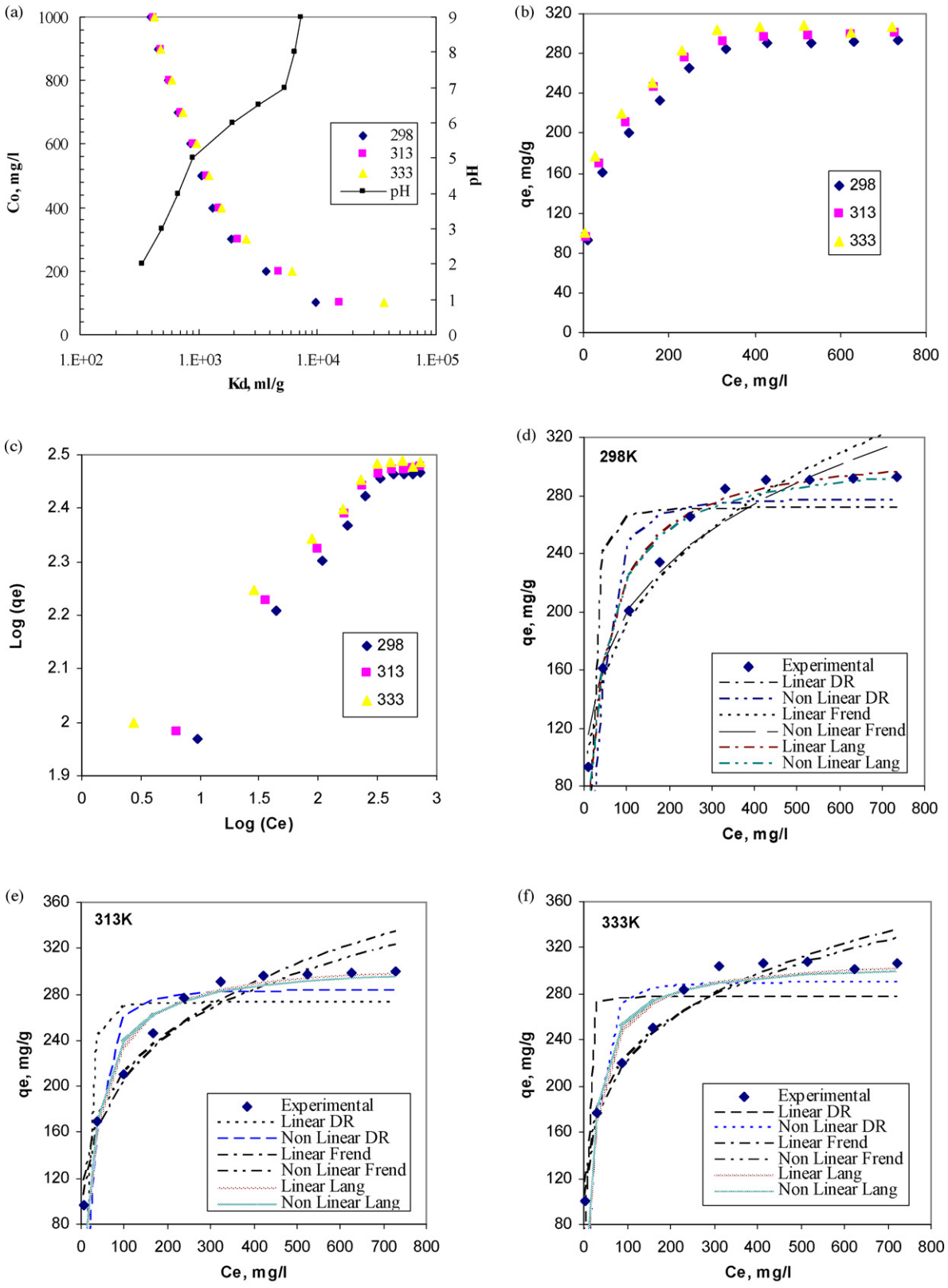

Fig. 3. Sorption isotherm analysis for Sr^{2} on zeolite Na A–X blend at three studied temperatures (a) effect of initial concentration and pH on the distribution coefficients, (b) equilibrium isotherms, (c) linear Freundlich isotherm, (d–f) linear and non-linear fitting of Freundlich, D–R, Langmuir equations.

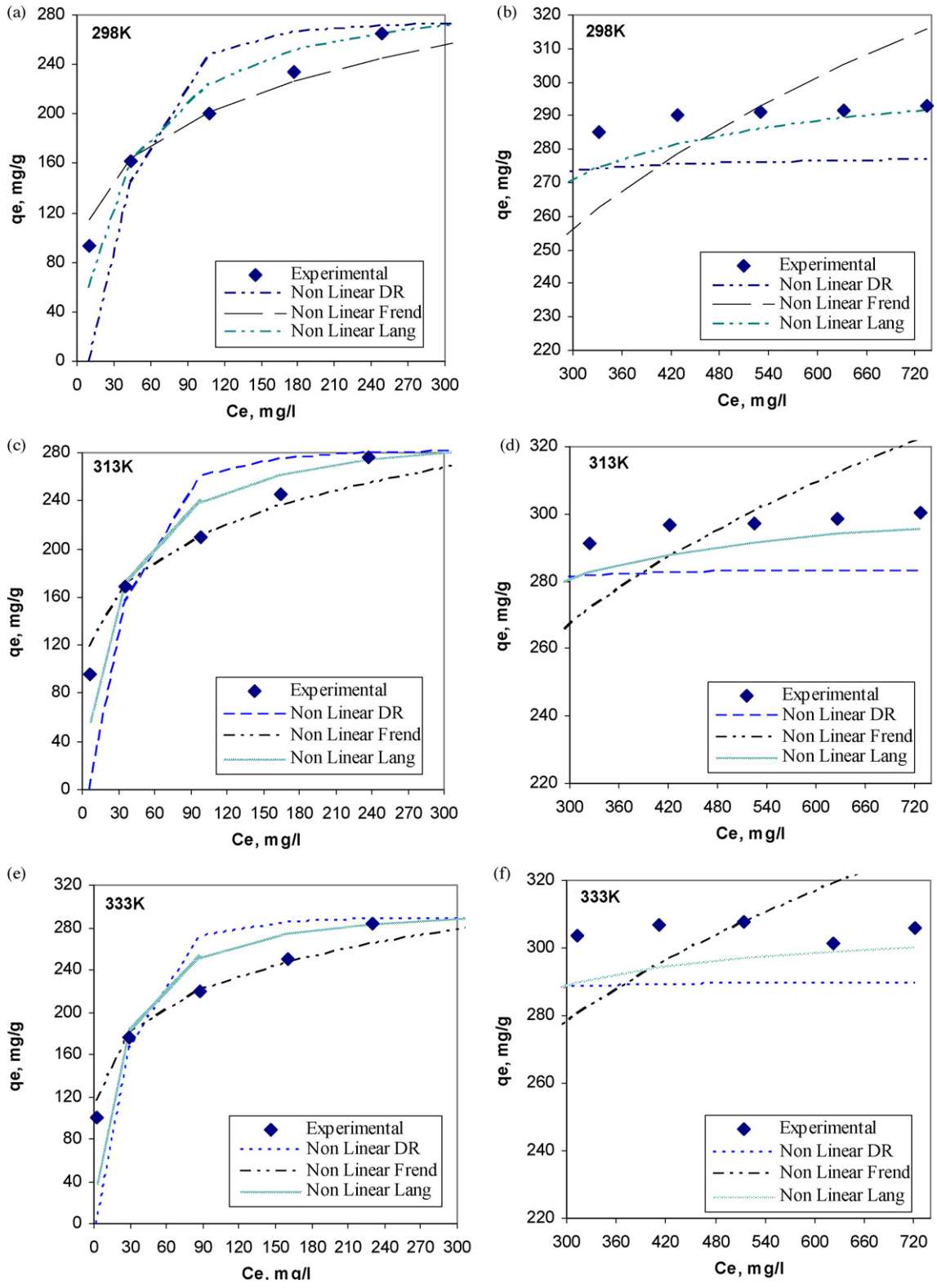

Fig. 4. Examination of the behavior of experimental isotherm data for sorption of Sr^2 on zeolite Na A–X blend at three different studied temperatures using non-linear D–R, Freundlich and Langmuir models.

isotherm parameters [44–47]. To assess the nature of the zeolite surface, the experimental data were fitted to the linear form of Freundlich isotherm. This isotherm is an empirical equation employed to describe the interaction between the sorbed molecules and heterogeneous systems and suggests that sorption energy exponentially decreases on completion of the sorption centers of a sorbent and the non-linear form is expressed by the following equation [44,48]:

$$q_e = K_f C_e^{1/n} \quad (14)$$

Table 4
Results of linear regression of the experimental data to different two parameters isotherms for Sr^{2+} sorbed onto zeolite Na A–X blend.

Model	Equation	Parameter	Temperature (K)		
			298	313	333
Freundlich isotherm	$\log q_e = \log K_f + \frac{1}{n}\log C_e$	n	3.73	4.12	4.80
		K_f	55.69	67.22	85.27
		R^2	0.964	0.964	0.974
Langmuir isotherm	$R_L = \frac{1}{1+bC_o}$	b	0.024	0.031	0.042
		Q^o	312.5	312.5	312.5
	$\frac{C_e}{q_e} = \frac{1}{Q^o b} + \frac{1}{Q^o}C_e$	R_l	0.45–0.04	0.39–0.03	0.31–0.02
		R^2	0.987	0.998	0.998
D–R isotherm	$\ln q_e = \ln q_m - \beta\varepsilon^2$	q_m	271.4	275.7	277
		b	0.005	0.003	0.001
	$E = (-2\beta)^{-1/2}$	R^2	0.870	0.863	0.821

the linear form is given by [44,48]:

$$\log q_e = \log K_f + \left(\frac{1}{n}\right)\log C_e \tag{15}$$

where K_f the Freundlich constant (mg/g).

The visual examination of the results, Fig. 3c, suggests that the sorption of Sr^{2+} onto zeolite Na A–X blend obeys Freundlich isotherm up to nearly initial concentration (500 mg/l) then a considerable deviation is noticed. Table 4 shows the results of fitting whole range of the experimental data to the model, it is clearly shown that the correlation coefficients have high values indicating that the zeolite surface is heterogeneous. The values of Freundlich intensity constant (n) are greater than unity and less than 10 for Sr^{2+}. These values suggest that the proposed backfill shows an increased tendency for sorption with increasing solid phase concentration. The numerical values of the sorption capacity (K_f) are presented in Table 4, the sorption capacity increases by increasing the ambient temperature.

Dubinin–Radushkevich (D–R) isotherm is applied to find out the sorption mechanism based on the potential theory assuming heterogeneous surface. The model is expressed as [46]:

$$q_e = q_m \exp\left(\frac{(RT\ln(1+1/C_e))^2}{-2E^2}\right) \tag{16}$$

The linear form of the model is given by:

$$\ln q_e = \ln q_m - \beta\varepsilon^2 \tag{17}$$

$$E = (-2\beta)^{-1/2} \tag{18}$$

where q_m is the maximum amount of ion that can be sorbed onto unit weight of zeolite (mg/g), β constant related to sorption energy (mol^2/kJ^2), ε is the polanyi potential = $RT\ln(1+1/C_e)$, where R is the gas constant (kJ/mol K), and T is the absolute temperature (K), and E is the mean free energy of the sorption (kJ/mol). Linear regression analysis using paired of $\ln q_e$ and ε^2 (Eq. (17)) resulted in the derivation of q_m, β, E and the correlation factor (R^2). The examination of the results revealed that correlation between this model and the experimental data is respectively week compared with that of Freundlich model. The values of D–R parameters are presented in Table 4. The maximum sorption capacities of zeolite (q_m) is in the ranges of 271–277 mg/g for Sr^{2+}.

Langmuir isotherm model is based on the assumptions that the sorption takes place at specific homogenous sites within the adsorbent, the adsorbent has a finite capacity for the sorbate and that all sites are identical and energetically equivalent because the sorbent is structurally homogeneous [45]. The equation of Langmuir is represented as follows:

$$q_e = \frac{Q^o bC_e}{1+bC_e} \tag{19}$$

The linear form of equation is given by:

$$\frac{C_e}{q_e} = \frac{1}{Q^o b} + \frac{1}{Q^o}C_e \tag{20}$$

$$R_L = \frac{1}{1+bC_o} \tag{21}$$

where Q^o is the monolayer sorption capacity (mg/g), b is the Langmuir constant, and R_L is the equilibrium parameter constant. The results of fitting the experimental data to the linear form of Langmuir model (Table 4) illustrate high values of the correlation coefficients (R^2) that indicate that this model provide a good representation of the experimental data. The value of equilibrium parameter (R_L) indicates the type of isotherm to be irreversible ($R_L = 0$), favorable ($0 < R_L < 1$), linear ($R_L = 1$), or unfavorable ($R_L > 1$). The ranges of R_L values (Table 4) were found to be less than 1 and greater than 0 indicating the favorable sorption isotherms of Sr^{2+} onto zeolite. The numerical value of monolayer sorption capacity

Table 5
Results of the non-linear regression of the experimental data to different isotherms for Sr^{2+} sorbed onto zeolite Na A–X blend.

Model	Equation	Parameter	Temperature (K)		
			298	313	333
Freundlich isotherm	$q_e = K_f C_e^{1/n}$	n	4.3	4.74	5.37
		K_f	68.03	80.47	96.25
		Error	0.024	0.021	0.018
		R^2	0.947	0.949	0.952
Langmuir isotherm	$q_e = \frac{Q^o bC_e}{1+bC_e}$	b	0.025	0.035	0.050
		Q^o	307.38	307.54	308.55
		Error	0.0049	0.008	0.017
		R^2	0.947	0.933	0.867
D–R isotherm	$q_e = q_m \exp\left(\frac{(RT\ln(1+1/C_e))^2}{-2E^2}\right)$	q_m	271.4	275.7	277
		b	0.005	0.003	0.001
		R^2	0.870	0.863	0.821

Table 6
Results of the non-linear regression of the experimental data to different isotherms for Sr^{2+} sorbed onto zeolite Na A–X blend.

Model	Equation	Parameter	Temperature (K)		
			298	313	333
Freundlich isotherm	$q_e = K_f C_e^{1/n}$	n	3.27	3.58	4.35
		K_f	48.47	59.45	79.38
		R^2	0.995	0.996	0.996
D–R isotherm	$q_e = q_m \exp\left(\frac{(RT\ln(1+1/C_e))^2}{-2E^2}\right)$	q_m	294.8	302.6	305.4
		b	0.006	0.005	0.002
		E	9.12	10.0	15.81
		R^2	0.95	0.963	0.921

(Q^o) and the free energy of adsorption constant (b) evaluated form the slope and intercept of C_e/q_e versus C_e are given in Table 4. The value of the saturation capacity (Q^o) corresponds to monolayer coverage and defines the total capacity of the zeolite for a specific ion. Langmuir model supposed that the saturation capacity (Q^o) is coincided with saturation of a fixed number of identical surface sites, so the values of (Q^o) should be independent on temperature. But it should be noted that various reported studies indicate that small to modest increase or decrease in the saturation capacity with increasing the temperature were observed that are due to the association of the sorption to surface functional group rather than a set of identical surface sites [49–52]. As observed from Table 4, the value of the saturation capacity is constant independent on the temperature where the results of the kinetic analysis and effect of pH revealed that the sorption process take place on surface functional group rather than a set of identical surface sites.

Due to the violation between the results obtained from fitting the experimental data to the linear form of Langmuir model and that revealed from the kinetic studies, the experimental data were fitted to the non-linear forms of Freundlich, D–R and Langmuir equations. The calculated parameters from the linear fitting were used as initial guess to the non-linear fitting to reduce the execution time. Fig. 3d–f illustrates the experimental, non-linear and linear fitted isotherm data by the studied models at the three studied temperatures and the results are listed in Table 5. From the visual examination of these plots, it is clearly shown that fitting the data to Freundlich model produce overestimated values for the amount of Sr^{2+} sorbed onto zeolite Na A–X blend where the other two models will produce underestimated values. Also, it is noted that the non-linear fitting results are closer to the experimental data. This remark is consistence with other reported studies that indicate that the transformation of the non-linear isotherm equations to linear form implicitly alter their error structure and may also violate the error variance and normality assumption of standard least squares [48,53–55].

The results in Fig. 4a–f depicted that the behavior of the experimental isotherm data could be divided into two trends; the limit of each trend was determined using a trial and error procedure to maximize the correlation coefficients (R^2). It was found that the first trend includes Sr^{2+} concentration sorbed onto zeolite Na A–X blend from nearly 80–280 mg/g and the second trend from 280 to the saturation value. The first trend fit better to Freundlich model where the second trend fit better to the Langmuir and D–R model. This might be attributed to the fact that with progressive surface coverage of zeolite at intermediate concentrations, the attractive forces between the radionuclides such as van der Waals forces, increases more rapidly than the repulsive forces, exemplified by short-range electronic or long-range Coulombic dipole repulsion, and consequently, the radionuclides manifest a stronger tendency to bind to the zeolite site [48]. Where at the high concentration values, the zeolite approach its saturation capacity.

The first trend was fitted to the non-linear Freundlich isotherm equation and the second trend fitted to both non-linear Langmuir and D–R equations, the results indicate that the data fit Freundlich and D–R better (Table 6). This confirms that the sorption occur on the heterogeneous surface of the zeolite, the value of the equilibrium values estimated from D–R are nearly equal to that of the experimental data. The mean free energy values of the sorption are in the range of 8–16 k/mol, this confirm that the sorption is controlled by ion exchange mechanism.

3.4. Thermodynamic studies

Based on fundamental thermodynamics concept, it is assumed that in an isolated system, energy cannot be gained or lost and the entropy change is the only driving force. In environmental engineering practice, both energy and entropy factors must be considered in order to determine if the sorption process will occur spontaneously. Gibbs free energy change, ΔG^o, is the fundamental criterion of spontaneity. Reactions occur spontaneously at a given temperature if ΔG^o is a negative quantity. The values of thermodynamic equilibrium constant at different studied temperatures were determined from the plot of $\ln(q_e/C_e)$ versus q_e[56]. The variation of K_c with temperature, as summarized in Table 7, showed that K_c values increase with increase in sorption temperature, thus implying a strengthening of adsorbate–adsorbent interactions at higher temperature. Also, the obtained negative values of ΔG^o confirm the feasibility of the process and the spontaneous nature of the sorption processes. Other thermal parameters such as enthalpy change (ΔH^o), and entropy change (ΔS^o) were also calculated. The values of enthalpy change (ΔH°) and entropy change (ΔS^o), calculated from the slope and intercept of the plot of $\ln K_c$ versus $1/T$ (figure omitted) are also given in Table 7. The change in ΔH^o for Sr^{2+} in zeolite Na A–X blend was found to be positive confirming the endothermic nature of the sorption processes. ΔS^o values were found to be positive due to the exchange of the Sr^{2+} ions with more mobile ions present on the sorbent, which would cause increase in the entropy during the sorption process.

Table 7
Values of thermodynamic parameters for sorption of Sr^{2+} ions onto zeolite Na A–X.

Temperature (K)	K_c	ΔG^o (kJ/mol)	R^2	ΔH^o (kJ/mol)	ΔS^o (J/mol K)
298	10.5	−5.83	0.96	1.44	0.024
313	11.16	−5.98	0.97		
33	11.2	−5.99	0.96		

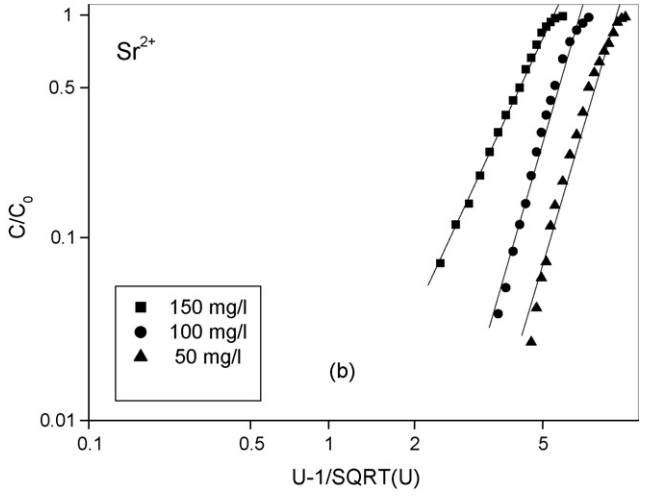

Fig. 5. Plots of $U - 1/\sqrt{U}$ versus C/C_o for Sr^{2+} at three feed concentration (50, 100, 150 mg/l) on linear probability scale.

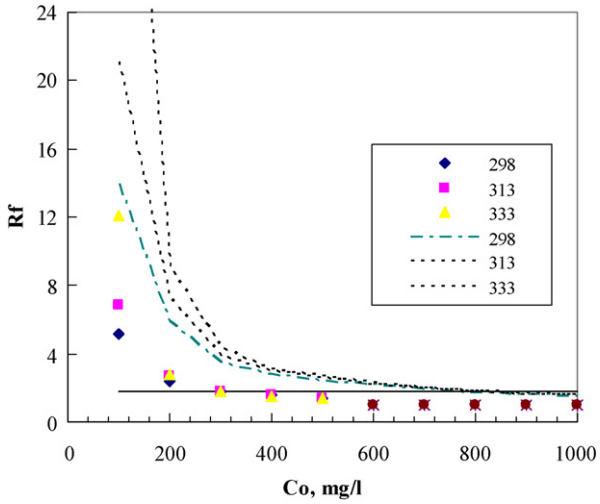

Fig. 6. Variation in the retardation coefficient as a function of initial concentration at three studied temperatures.

3.5. Column experiment and construction of breakthrough curves

To determine the hydrodynamic dispersion coefficient in laboratory, the result of the column studies were reported in terms of effluent pore volume variable ($U = (vt/\theta)$). Fig. 5 illustrates the effluent relative concentration, C/C_o as a function of $(U - 1)/\sqrt{U}$ on linear probability scale. As shown from the figure, the measured experimental data could be presented as straight lines and the values of the hydrodynamic dispersion coefficient were calculated using the following equation:

$$D_L = \frac{vL}{8}\left(\left.\frac{U-1}{\sqrt{U}}\right|_{0.84} - \left.\frac{U-1}{\sqrt{U}}\right|_{0.16}\right)^2 \quad (22)$$

The values of the hydrodynamic dispersion were found to be 0.064, 0.212, and 0.296 (m^2/y).

3.6. Assessment of the barrier performance

To assess the performance of the prepared zeolite as a backfill a simple analytical model was used. To derive the analytical model, it was assumed that the backfill is porous, homogeneous, isotropic, saturated; and the flow reached steady state so Darcy's law was applied. The one-dimensional advection–dispersion equation for a reactive contaminant is given below [57]:

$$\frac{\partial C}{\partial t} + \frac{\rho}{\theta}\frac{\partial q}{\partial t} = D\frac{\partial^2 C}{\partial x^2} - v\frac{\partial C}{\partial x} \quad (23)$$

By introducing the concentration in the in liquid phase in the term $((\rho/\theta)(\partial q/\partial t))$, the following equation is obtained:

$$\frac{\partial C}{\partial t} + \frac{\rho}{\theta}\frac{\partial q}{\partial C}\frac{\partial C}{\partial t} = D\frac{\partial^2 C}{\partial x^2} - v\frac{\partial C}{\partial x} \quad (24)$$

$$R_f\frac{\partial C}{\partial t} = D\frac{\partial^2 C}{\partial x^2} - v\frac{\partial C}{\partial x} \quad (25)$$

where

$$R_f = \left(1 + \frac{\rho}{\theta}\frac{\partial q}{\partial C}\right)$$

The results obtained from the analysis of the sorption equilibrium data were used to quantify the retardation coefficient of Sr^{2+} onto zeolite Na A–X blend. In this respect to the derivative of Freundlich equation with respect to the Sr^{2+} concentration in the groundwater up to 500 mg/l initial concentration and D–R equation derivative from 500 mg/l initial concentration were utilized to determine the retardation coefficient as follow:

$$R_f = \begin{cases} 1 + \dfrac{\rho K_f}{\theta n} C^{1/n-1} & 100\,\text{mg/g} \prec C \prec 500\,\text{mg/g} \\ 1 + \dfrac{\rho RTq_m E^2}{\theta}\exp\left(\dfrac{(RT\ln(1+1/C))^2}{2E^2}\right)\ln\left(\dfrac{C+1}{C}\right)\left(\dfrac{1}{C+1}\right)\left(\dfrac{1}{C}\right) & 500\,\text{mg/g} \prec C \prec 1000\,\text{mg/g} \end{cases} \quad (26)$$

The variation in the retardation coefficient as a function of initial concentration at different temperatures using Eq. (26) are illustrated in Fig. 6 (scatter pattern), at low concentration the effect of temperature on the retardation coefficient is very obvious. As the initial concentration increase this effect become negligible approaches a constant value of 1. Another way to determine the retardation coefficient is to use the distribution coefficients $(1 + (\rho/n)K_d)$, the distribution coefficients could be determined either from fitting the experimental isotherm data to linear isotherm model (solid line) or from dividing the amount sorbed on the remaining concentration in the groundwater (q_e/C_e) dotted line pattern. Fig. 6 presents a comparison between the retardation coefficients obtained from the above mention methods, as shown in the figure the retardation coefficient calculated from using (q_e/C_e) to estimate the distribution coefficient give the highest values for the retardation coefficient.

The integration of the governing Eq. (24) using specific boundary conditions for the system of interest, provides a number of analytical solutions. Some of these solutions have been derived for one-dimensional pulse contaminant input or a continuous input [58].

$$C(x,t) = \frac{C_o}{\sqrt{4\pi D_r t}}\exp\left(-\frac{(x - v_r t)^2}{4D_r t}\right) \quad (27)$$

To assess the effect of the utilized method to determine the retardation coefficients on the prediction of Sr concentration, the values of the hydrodynamic dispersion coefficient, the water velocity and the distance were fixed at constant values. Fig. 7 shows the

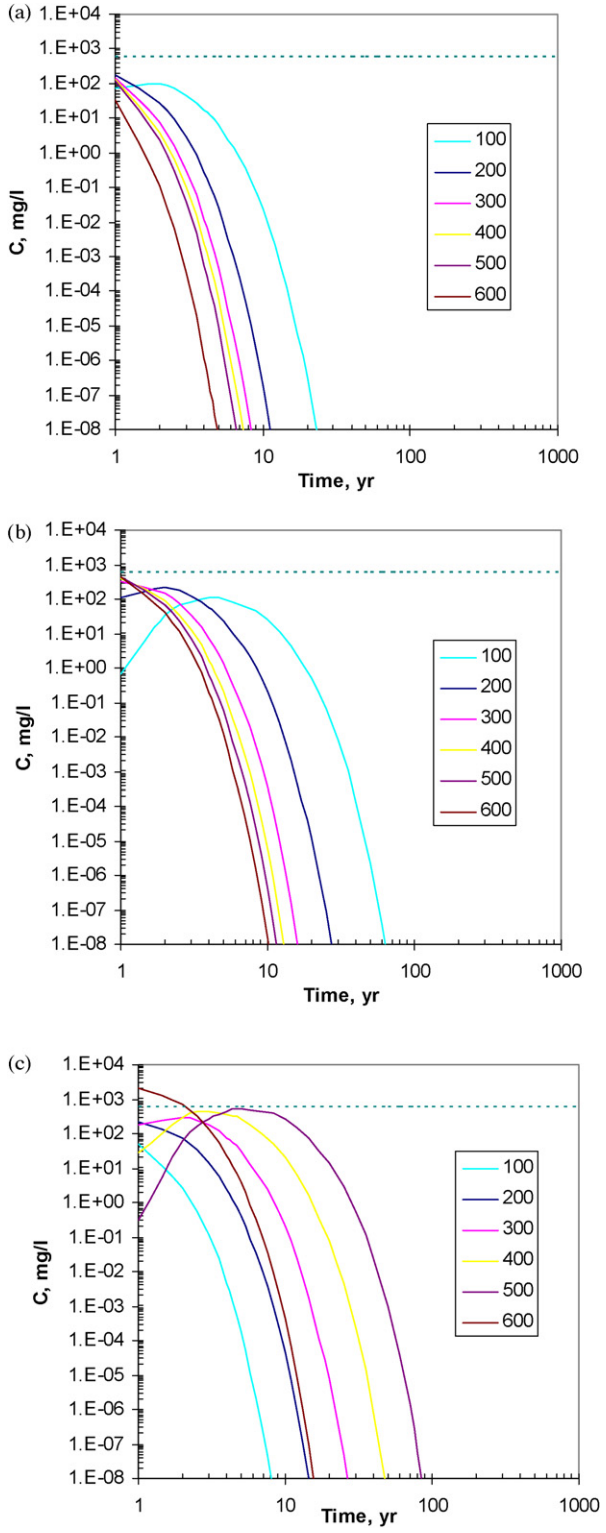

Fig. 7. Effect of the calculation of retardation coefficient method on the Sr concentration as a function of time using (a) Eq. (26), (b) (q_e/C_e), and (c) linear isotherm model.

effect of the method to determine the retardation coefficients on the predication of the concentration as a function of time. A considerable effect is noticed between the predicted concentration values (Fig. 7a–c), the utilization of the distribution coefficient values to determine the retardation coefficients will over estimate the predicted concentration. This might lead to a conservative design that reduces the amount of the waste disposed in the disposal facility. A greater care should be given to the estimation of the retardation confident for low inventory.

4. Conclusion

The technical feasibility of using zeolite Na A–X as sorbing barrier was examined by evaluating sorption characteristics of Sr^{2+} onto the prepared zeolite. The results illustrate the controlling sorption mechanism, the sorption isotherm and the thermodynamic parameters. The specific conclusions pertaining to the results presented herein can be drawn as follow:

(1) From the examination of the effect of contact time it was found that the sorption of Sr^{2+} is due to two trends. At the first trend the amount of sorbed strontium increases sharply with time and then gradually increases to reach an equilibrium value in approximately 90 min.
(2) To determine the controlling mechanisms, the experimental data were analyzed using four kinetic model equations. The results of the analysis indicate that the sorption of Sr^{2+} onto the proposed backfill is a chemisorption process and that within the first 30 min the sorption might be proceeded by diffusion. The intraparticle diffusion and boundary layer effect were found to be the controlling mechanisms Also it was found that as the concentration increase the boundary layer effect will be greater.
(3) The suitability of the geochemical conditions was preliminarily assessed by conducting equilibrium sorption studies at different pH ranging from 2.0 to 9.0, It was observed that the values of the Sr^{2+} distribution coefficients (k_d) increases as the groundwater pH increase and nearly reaches a plateau at pH 6. This reflects that the material is showing a reasonable retention performance at the mean groundwater pH.
(4) To optimize the design of the barrier, the effect of the initial concentration on the retention of Sr^{2+} on the zeolite Na A–X blend at three temperatures was investigated. At high initial concentration range the effect of ambient temperature on the assessment of the distribution coefficients is negligible. Where at lower initial concentration, as the ambient temperature increases the distribution coefficients will increase.
(5) Due to the violation between the results obtained from fitting the experimental data to the linear form of Langmuir model and that revealed from the kinetic studies, the experimental data were fitted to the non-linear forms of Freundlich, D–R and Langmuir equations. The results of non-linear fitting are closer to the experimental data. This was attributed to the fact that the transformation of the non-linear isotherm equations to linear form implicitly alters their error structure and may also violate the error variance and normality assumption of standard least squares.
(6) The experimental isotherm data were found to be best described by Freundlich isotherm up to 500 mg/l initial concentration then the data are best described using D–R model.
(7) The analysis of the isotherm data confirms that the sorption occur on the heterogeneous surface of the zeolite, the value of the equilibrium values estimated from D–R are nearly equal that of the experimental data, the mean free energy values of the sorption is in the range of 8–16 k/mol, this confirm that the sorption is controlled by ion exchange.
(8) From the thermodynamic analysis the endothermic nature of the sorption processes was confirmed, and it was found that the exchange of the Sr^{2+} ions with more mobile ions present on the sorbent, which would cause increase in the entropy during the sorption process. Negative values of ΔG^o confirm the feasibility of the process and the spontaneous nature of the sorption processes

(9) To assess the effect of the utilized method to determine the retardation coefficients on the predicted concentration, a simple pulse analytical model was used. It was concluded that the prediction of the concentration was found to be highly affected by the method utilized to determine the retardation coefficient.

(10) Generally the utilization of the distribution coefficient values to determine the retardation coefficients will produce overestimated values for the predicted concentration. This might lead to a conservative design that reduces the amount of the waste disposed in the disposal facility. A greater care should be given to the estimation of the retardation confident for low inventory.

References

[1] Strontium-90, http://en.wikipedia.org/wiki/Strontium-90.
[2] International Atomic Energy Agency, Scientific and technical basis for the near surface disposal of low and intermediate level waste, Technical Report Series No. 412, International Atomic Energy Agency, Vienna, 2002.
[3] A.E. Osmanlioglu, Treatment of radioactive liquid waste by sorption on natural zeolite in Turkey, J. Hazard. Mater. 137 (2006) 332–335.
[4] A.M. El-Kamash, Evaluation of zeolite A for the sorptive removal of Cs^+ and Sr^{2+} ions from aqueous solutions using batch and fixed bed column operations, J. Hazard. Mater. 151 (2008) 432–445.
[5] K.M. Abdel Rahman, A.M. El-Kamash, M.R. El-Sourougy, N.M. Abdel Moniem, Thermodynamic modeling for the removal of Cs^+, Sr^{2+}, Ca^{2+}, and Mg^{2+} ions from aqueous waste solution using zeolite A, J. Radioanal. Nucl. Chem 268 (2006) 221–230.
[6] A.M. El-Kamash, A.A. Zaki, M. Abd El Geleel, Modeling batch kinetics and thermodynamics of zinc and cadmium ions removal from waste solutions using synthetic zeolite A, J. Hazard. Mater. 127 (2005) 211–220.
[7] A. Dyer, A.S. Abdel Gawad, M. Mikhail, H. Enamy, M. Afshang, The natural zeolite, laumontite, as a potential material for the treatment of aqueous nuclear wastes, A, J. Radioanal. Nucl. Chem. 4 (1991) 265–276.
[8] A.M. El-Kamash, M.R. El-Nagger, M.I. El-Dessouky, Immobilization of cesium and stronium radionuclides in zeolite–cement blends, J. Hazard. Mater. 136 (2006) 310–316.
[9] A. Dyer, T. Las, M. Zubair, The use of natural zeolite for radioactive waste treatment studies on leaching from zeolite–cement composites, J. Radioanal. Nucl. Chem. 243 (2001) 839–841.
[10] A. Kaya, S. Durukan, Utilization of bentonite-embedded zeolite as clay liner, Appl. Clay Sci. 25 (2004) 83–91.
[11] K. Kayabalı, Engineering aspects of a novel landfill material: bentonite amended natural zeolite, Eng. Geol. 46 (1997) 105–114.
[12] H.A. Ibrahium, A.M. El-Kamash, M. Hanafy, N.M. Abdel Monem, Examination of the use of synthetics zeolite Na-AX blends as backfill material in a radioactive waste disposal facility, J. Chem. Eng. 144 (2008) 67–74.
[13] R.O. Abdel Rahman, H.A. Ibrahim, N.M. Abdel Monem, Long-term performance of zeolite Na A–X blend as backfill material in near surface disposal vault, Chem. Eng. J. 149 (2009) 143–152.
[14] H.A. Ibrahium, Evaluation of using synthetic zeolite as a backfill material in radioactive waste disposal facility, Ph.D. Thesis, Chemical Engineering Department, Faculty of Engineering, Cairo University, 2009.
[15] A. Nilchi, B. Maalek, A. Khanchi, M. Ghanadi Maragheh, A. Bagheri, K. Savoji, Ion exchangers in radioactive waste management: natural Iranian zeolites, Appl. Radiat. Isot. 64 (2006) 138–143.
[16] D.V. Marinin, G.N. Brown, Studies of sorbent/ion-exchange materials for the removal of radioactive strontium from liquid radioactive waste and high hardness groundwater, Waste Manage. 20 (2000) 545–553.
[17] M.M. Askarieh, S.V. Worth, Post-closure thermal evolution of a conceptual repository design for the disposal of intermediate-level radioactive waste, in: Proceedings ENS TOPSEAL'99 Meeting on 'Commitment to the Future Environment', vol. II, Poster Presentation, 10–14 October 1999, Antwerp, Belgium, Belgian Nuclear Society, 1999, ISBN 3-9520691-4-0.
[18] B.H. Hameed, I.A.W. Tan, A.L. Ahmad, Adsorption isotherm, kinetic modeling and mechanism of 2,4,6-trichlorophenol on coconut husk-based activated carbon, Chem. Eng. J. 144 (2008) 235–244.
[19] Y.S Ho, G. McKay, Pseudo-second order model for sorption processes, Process Biochem. 34 (1999) 451–465.
[20] G. McKay, Y.S. Ho, The sorption of lead (II) on peat, Water Res. 33 (1999), 587-585.
[21] G. McKay, Y.S. Ho, Pseudo-second order model for sorption rocesses, Process Biochem. 34 (1999) 451–460.
[22] F. Helfferich, Ion Exchange, McGraw Hill, New York, 1962.
[23] G.E. Boyd, A.W. Adamson, L.S. Mayers, The exchange adsorption of Ions from aqueous solutions by zeolites. II. Kinetics, J. Am. Chem. Soc. 69 (1947) 28–36.
[24] W.J. Weber, J.M. Morris, J. Sanit, Eng. Div. Am. Soc. Eng. 89 (1963) 31–39.
[25] B. Fonseca, H. Maio, C. Quintelas, A. Teixeira, T. Tavares, Retention of Cr(VI) and Pb(II) on a loamy sand soil Kinetics, equilibria and breakthrough, Chem. Eng. J. 152 (2009) 212–219.
[26] Grégorio Crini, Harmel Ndongo Peindy, Frédéric Gimbert, Capucine Robert, Removal of C.I. Basic Green 4 (Malachite Green) from aqueous solutions by adsorption using cyclodextrin-based adsorbent: kinetic and equilibrium studies, Sep. Purif. Technol. 53 (2007) 97–110.
[27] G. Crini, P. Badot, Application of chitosan, a natural aminopolysaccharide, for dye removal from aqueous solutions by adsorption processes using batch studies: a review of recent literature, Prog. Polym. Sci. 33 (2008) 399–447.
[28] W. Plazinski, W. Rudzinski, A. Plazinska, Theoretical models of sorption kinetics including a surface reaction mechanism: a review, Adv. Colloid Interface Sci., in press, doi:10.1016/j.cis.2009.07.009.
[29] V.C. Taty-Costodes, H. Fauduet, C. Porte, A. Delacroix, Removal of Cd(II) and Pb(II) ions, from aqueous solutions, by adsorption onto sawdust of *Pinus sylvestris*, J. Hazard. Mater. 105 (2003) 121–142.
[30] K.S. Hui, C.Y.H. Chao, S.C. Kot, Removal of mixed heavy metal ions in wastewater by zeolite 4A and residual products from recycled coal fly ash, J. Hazard. Mater. B127 (2005) 89–101.
[31] E.S. Dragan, M.V. Dinu, D. Timpu, Preparation and characterization of novel composites based on chitosan and clinoptilolite with enhanced adsorption properties for Cu^{2+}, Bioresour. Technol. 101 (2010) 812–817.
[32] A.R. Cestari, E.F.S. Vieira, A.A. Pinto, E.C.N. Lopes, Multiple adsorption of anionic dyes on silica/chitosan hybrid 1. Comparative kinetic data from liquid- and solid-phase models, J. Colloid Interface Sci. 72 (2005) 292–363.
[33] S.K. Alpat, O. Ozbayrak, S. Alpat, H. Akçay, The adsorption kinetics and removal of cationic dye, toluidine blue O, from aqueous solution with Turkish zeolite, J. Hazard. Mater. 151 (2008) 213–220.
[34] M.E. Argun, Use of clinoptilolite for the removal of nickel ions from water: kinetics and thermodynamics, J. Hazard. Mater. 150 (2008) 587–595.
[35] A.-H. Chen, S.-C. Liu, C.-Y. Chen, C.-Y. Chen, Comparative adsorption of Cu(II), Zn(II), and Pb(II) ions in aqueous solution on the crosslinked chitosan with epichlorohydrin, J. Hazard. Mater. 154 (2008) 184–191.
[36] A. Günay, E. Arslankaya, I. Tosun, Lead removal from aqueous solution by natural and pretreated clinoptilolite: adsorption equilibrium and kinetics, J. Hazard. Mater. 146 (2007) 362–371.
[37] Z. Reddad, C. Gerente, Y. Andres, P. Le Cloirec, Adsorption of several metal ions onto a low-cost biosorbent: kinetic and equilibrium studies, Environ. Sci. Technol. 36 (2002) 2067–2073.
[38] N.A. Oztas, A. Karabakan, Topal, Removal of Fe(III) ion from aqueous solution by adsorption on raw and treated clinoptilolite samples, Micropor. Mesopor. Mater. 111 (2008) 200–205.
[39] A.M. El-Kamash, B. El-Gammal, A.A. El-Sayed, Preparation and evaluation of cerium (IV) tungstate powder as inorganic exchanger in sorption of cobalt and europium ions from aqueous solutions, J. Hazard. Mater. 141 (2007) 719–728.
[40] Performance of engineered barrier materials in near surface disposal facilities for radioactive waste, IAEA-TECDOC-1255, November 2001, appendix 10.
[41] D. Kavitha, C. Namasivayam, Experimental and kinetic studies on methylene blue adsorption by coir pith carbon, Bioresour. Technol. 98 (2007) 14–21.
[42] E. Skwarek, M. Matysek–Nawrocka, W. Janusz, V.I. Zarko, V.M. Gun'ko, Adsorption of heavy metal ions at the al2o3-sio2/naclo4 electrolyte interface, Physicochem. Prob. Miner. Process. 42 (2008) 153–164.
[43] K.F. Hayes, L.E. Katz, Application of X-ray absorption spectroscopy for surface complexation modeling of metal ion sorption, in: P.V. Brady (Ed.), Physics and Chemistry of Mineral Surfaces, CRC Press, New York, 1996, pp. 147–224.
[44] H.M.F. Freundlich, Over the adsorption in solution, J. Phys. Chem. 57 (1906) 385–470.
[45] I. Langmuir, The adsorption of gases on plane surfaces of glass, mica and platinum, J. Am. Chem. Soc. 40 (1918) 1361–1403.
[46] M.M. Dubinin, L.V. Radushkevich, Equation of the characteristic curve of activated charcoal, Chem. Zentr. 1 (1947) 875.
[47] J. Febriantoa, A.N. Kosasiha, J. Sunarso, Y.-H. Ju, N. Indraswati, S. Ismadji, Equilibrium and kinetic studies in adsorption of heavy metals using biosorbent: a summary of recent studies, J. Hazard. Mater. 162 (2009) 616–645.
[48] Y.S. Ho, J.F. Porter, G. Mckay, Equilibrium isotherm studies for the sorption of divalent metal ions onto peat: copper, nickel and lead Single component systems, Water Air Soil Poll. 141 (2002) 1–33.
[49] A.Y. Dursun, A comparative study on determination of the equilibrium, kinetic and thermodynamic parameters of biosorption of copper(II) and lead(II) ions onto pretreated Aspergillus niger, Biochem. Eng. J. 28 (2006) 187–195.
[50] X. Wang, Y. Qin, Z. Li, Biosorption of zinc from aqueous solutions by rice bran: kinetics and equilibrium studies, Sep. Sci. Technol. 41 (2006) 747–756, Metal removal: equilibrium and kinetics, Bioresour. Technol. 99 (2008) 1896–1903.
[51] V.J.P. Vilar, C.M.S. Botelho, R.A.R. Boaventura, Copper removal by algae Gelidium, agar extraction algal waste and granulated algal waste: kinetics and equilibrium, Bioresour. Technol. 99 (2008) 750–762.
[52] A.A. Zaki, M.I. Ahmad, R.O. Abdel Rahman, Evaluation of the Use of Natural Clay as a Barrier for the Retardation of Some Radionuclides, in the special issue on radioactive waste management science and technology for IJEES, in press.
[53] R.H. Myers, Classical and modern regression with applications, PWS-KENT (1990), pp. 297–298, 444–445.
[54] Y.-S. Ho, Selection of optimum sorption isotherm, Carbon 42 (2004) 2113–2130.
[55] Yuh-Shan Ho, Isotherms for the Sorption of Lead onto Peat: Comparison of Linear and Non-Linear Methods, Pol. J. Environ. Stud. 15 (1) (2006) 81–86.
[56] M.I. Panayotova, Kinetic and thermodynamic of copper ions removal from waste water by use of zeolite, Waste Manage. 21 (2001) 671–676.
[57] J. Bear, Dynamics of Fluids in Porous Media, Elsevier, New York, 1972.
[58] R.J. Watts, Hazardous Waste: Sources, Pathways, Receptors, Wiley, New York, 1998.